

TUNABLE BAND-PASS FILTER USING RF MEMS CAPACITANCE AND TRANSMISSION LINE

S. C. Saha^{1,4,*}, U. Hanke², H. Sagberg³, T. A. Fjeldly¹, and T. Sæther¹

¹Department of Electronics and Telecommunications (IET), Norwegian University of Science and Technology (NTNU), Trondheim NO-7491, Norway

²Institute for Microsystems Technology, Vestfold University College, Tønsberg 3103, Norway

³Department of Microsystems and Nanotechnology, SINTEF ICT, P. O. Box 124, Blindern, Oslo NO-0314, Norway

⁴Electronics and Nanoscale Engineering, University of Glasgow, G12 8LT, UK

Abstract—In this paper we present the design and fabrication of an RF MEMS tunable band-pass filter. The band-pass filter design uses both distributed transmission lines and RF MEMS capacitances together to replace the lumped elements. The use of RF MEMS variable capacitances gives the flexibility of tuning both the centre frequency and the band-width of the band-pass filter. A prototype of the tunable band-pass filter is realized using parallel plate capacitances. The variable shunt and series capacitances are formed by a combination of parallel plate RF MEMS shunt bridges and series cantilevers. The filter operates at C-X band. The measurement results agree well with the simulation results.

1. INTRODUCTION

Radio frequency micro electromechanical systems (RF MEMS) technology offers an attractive capability for RF systems, particularly in support of switching, variable capacitance and inductance and tuning functions [1–4]. One such component is the micro electromechanical voltage tunable capacitor, which can enable a wide

Received 6 July 2011, Accepted 25 August 2011, Scheduled 31 August 2011

* Corresponding author: Shimul Chandra Saha (shimul.saha@glasgow.ac.uk).

tuning range and high quality (Q) factors. Compared with solid state varactors, MEMS tunable capacitance and inductance have the advantage of lower loss, low voltage operation and potentially larger tuning range [1]. The interconnection loss and noise can also be less than off-chip solid state RF components. The actuation mechanism for MEMS capacitor is mostly electrostatic, consuming very little power during actuation. A parallel plate tunable capacitor can be fabricated using surface micromachining techniques. In standard filter design at low frequency, the MEMS varactor is used as a lumped element with off-chip inductors. At high frequency, some designs were reported with integrated transmission lines and MEMS capacitors [5, 6]. The transmission lines used for these designs are half wavelength or 180° , so the filter will be very long at low frequencies. The tuning range is also not very high for these filters, 3.8% and around 14%, respectively. Also, low-pass and band-pass filters integrating capacitive MEMS switches and short inductive transmission lines have been realized for frequencies above 10 GHz [7–9]. In [7], the change in cut-off frequency was obtained by switching different combinations of inductances and capacitances. In [8, 9], the cut-off and center frequencies were tuned by changing the inductance using MEMS switching. However, none of them had the capability of tuning bandwidth.

In this paper, we have presented a design of a band-pass filter with combination of low pass filter and high pass filter. The low pass filter was designed using the stepped impedance transmission line. A preliminary design of the low pass filter was presented in [10]. The low-pass filter was integrated with series coupling capacitors to obtain a 3rd order band-pass filter as presented in [11], is shown in Figure 1. A MEMS shunt capacitor was used to replace the low-impedance transmission line in a stepped impedance filter. The series inductor has been implemented using a short section of high impedance transmission line. The series capacitors work as a high-pass filter and

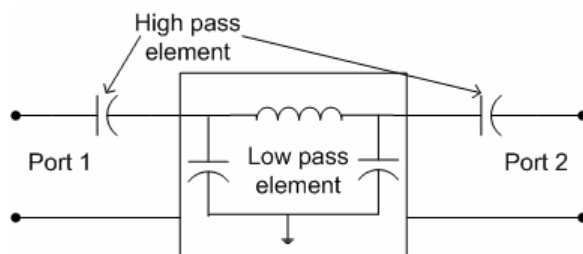


Figure 1. The basic band-pass filter, which is obtained from low and high pass combination.

are implemented using inline cantilever capacitive MEMS switches in series configuration. The tuning of both the center frequency and the bandwidth is possible by means of tunable capacitances. The presented band-pass filter is much more compact than filters based on half wave resonators. The center frequency of the band-pass filter can be tuned by shunt capacitors. The bandwidth of the filter can be tuned by changing the series capacitor. The filter has large tuning range, about 30% of its center frequency. Although step impedance filters don't have very sharp roll-off, they can still be useful for certain applications where compact size and wide tuning range are more important than the roll-off. The band-pass filter can be used in harmonic suppression in frequency synthesizer and transceiver system. The high tuning range and bandwidth tuning capability will be very useful in the systems operating in multiple frequencies and varying bandwidth.

Theory of capacitive switch, design of the band-pass filter consisting of a third-order 3dB ripple Chebyshev low-pass filter and series capacitances are described in Section 2. The filter was designed and optimized using the ADS[®] software from Agilent. A simulation of the filter performance is also presented in Section 2. A prototype of the filter is fabricated using our own facility at SINTEF MiNaLab, Oslo, Norway. Three ordinary parallel plate bridges were used as tunable shunt capacitances by actuating different combinations of the bridges. Series cantilevers of two different dimensions are used as series capacitors. The fabrication of the filter is presented in Section 3. The measurement results and re-simulation taking into account the effects of process constraints, are discussed in Section 4. Finally the paper is concluded.

2. THEORY, DESIGN AND SIMULATION

2.1. Theory of Parallel Plate Capacitance

A traditional parallel plate capacitor is shown in Figure 2. According to the theory presented in [11, 12], the value of the capacitance between the suspended bridge and center electrode for a deflection x from the initial position of the bridge can be determined by,

$$C(x) = \epsilon_0 \cdot \frac{A_e}{(g_0 - x) + \frac{t_d}{\epsilon_r}} \quad (1)$$

Here $A_e (L_e \times W_e)$ is the overlap area between the suspended beam and the bottom electrode, t_d is the thickness and ϵ_r is relative permittivity of the dielectric. L_e and W_e are length and width of the electrode respectively. g_0 is the initial gap between the suspended

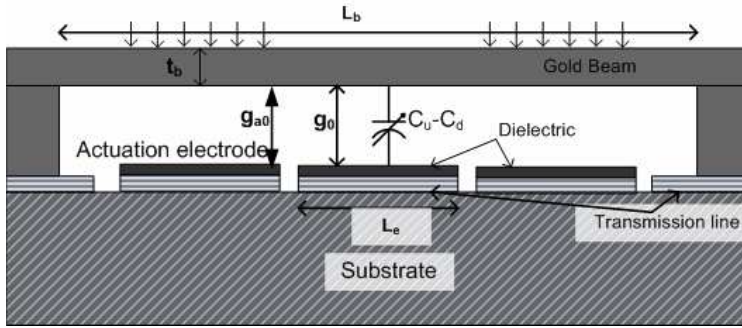


Figure 2. Side view of a traditional parallel plate capacitive switch in CPW configuration with separate actuation electrodes.

beam and bottom electrode. The deflection x is caused by the attractive electrostatic force F_e generated by the applied actuation voltage V_{DC} [12], i.e.,

$$F_e = \frac{1}{2} \frac{C_a(x) V_{DC}^2}{\left(g_{a0} - x + \frac{t_d}{\epsilon_r}\right)} \quad (2)$$

Here $C_a(x)$ is the total capacitance between the bridge and the actuation electrodes. For traditional parallel plate capacitance, the suspended beam can move up to one third of its initial position before it collapses to downstate. When $x = g_0$, the beam touches the centre electrode and the downstate capacitance becomes,

$$C_d = \epsilon_0 \epsilon_r \frac{A_e}{t_d} \quad (3)$$

Equation (3) is applicable for an ideal scenario, where both suspended beam and bottom dielectric surface are smooth. In practice, there may be some roughness present on the dielectric surface and also on the beam. The capacitance in this case is given by [12],

$$C_{dr} = \frac{\epsilon_0 A_e}{2} \left(\frac{1}{t_r + \frac{t_d}{\epsilon_r}} + \frac{\epsilon_r}{t_d} \right) \quad (4)$$

Here t_r is amplitude of the total roughness.

2.2. Theory of the Stepped-impedance Filter

It is well known [13,14], that if the length of the transmission line is short ($\beta l < \pi/4$) and the characteristic impedance is high the

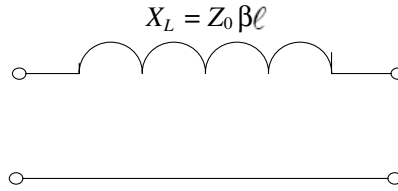


Figure 3. Equivalent circuit for short length and high characteristic impedance transmission line.

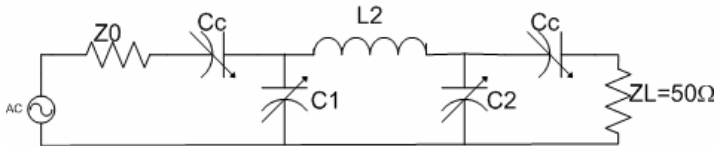


Figure 4. The band-pass filter topology.

transmission line can be represented by the equivalent circuit, as shown in Figure 3, where the reactance is given by,

$$X_L = Z_0 \beta \ell \tag{5}$$

Here the characteristic impedance of the line is Z_0 , the length is l and the propagation constant is β . So a series inductor can be represented by a short length of high characteristic impedance transmission line.

2.3. A Band Pass Filter with Third-order Low-pass Filter Topology and Optimization in ADS

A band pass filter topology, with 3rd order low pass filter and series capacitor is shown in Figure 4. The basic filter elements are extracted from the Chebyshev equal ripple low pass filter prototype [11, 13].

The normalized filter elements for a 3 dB ripple Chebyshev are given by $g_1 = 3.3487$, $g_2 = 0.7117$, $g_3 = 3.3487$, and $g_4 = 1.00$ is the load impedance [13]. A 3 dB ripple design is used to obtain a sharp roll-off above the cut-off frequency. A nominal center frequency of 5.8 GHz was chosen for this the filter, considering the use at C band. The proposed filter was fabricated on a 280 μm thick high resistivity silicon substrate. The relative dielectric constant of the substrate was 11.9 and the resistivity was 8000 $\Omega\text{-cm}$. For an 80 Ω CPW transmission line, the dimensions were 160 $\mu\text{m}/53 \mu\text{m}/160 \mu\text{m}$ (G/W/G). After tuning the filter performance in ADS [15], the nominal shunt and series capacitor and 80 Ω transmission length were optimized to 1.1 pF, 370 fF and 1467 μm (30.7°). Due to finite impedance, the high impedance

transmission line would introduce certain amount of shunt capacitance, and reduce the required amount shunt capacitance. A higher value of impedance, such as $100\ \Omega$ or more, could be chosen for the series inductance. This would make the transmission line very narrow, which may introduce high loss in the pass band. To compensate the loss, a very thick metal layer would require for transmission line.

2.4. Simulation of the Filter Performance, Tuning Centre Frequency and Bandwidth

A schematic view of the band pass filter with transmission line and MEMS capacitance are shown in Figure 5. The following parameters were used for simulation in ADS. The $80\ \Omega$ transmission line length was $1467\ \mu\text{m}$. The series capacitances in each side were $370\ \text{fF}$. The

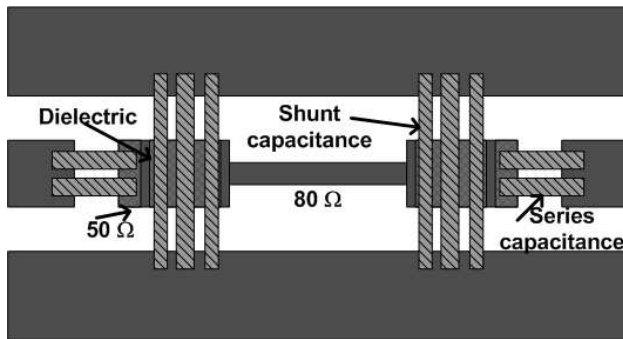


Figure 5. A 2D view of the proposed filter. For clarity the actuation electrode is not shown.

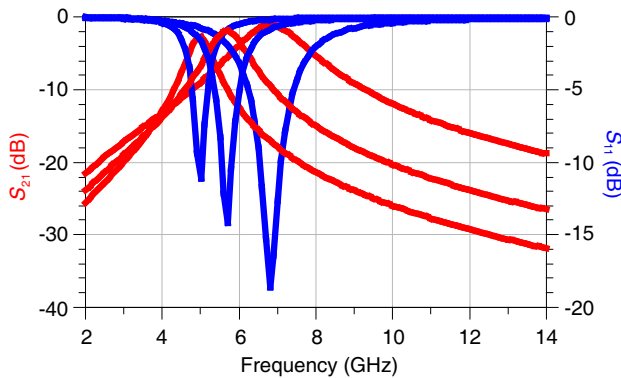


Figure 6. Tuning of center frequency by changing shunt capacitance.

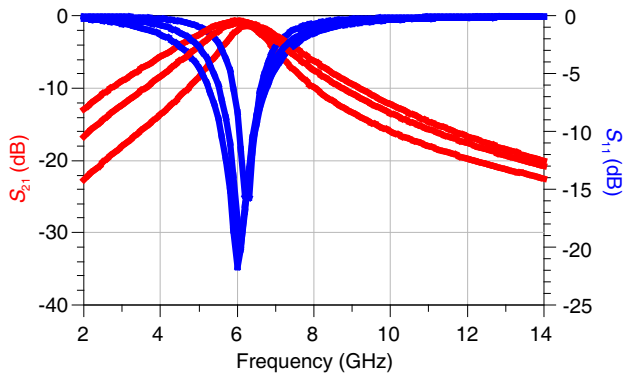


Figure 7. Tuning bandwidth by changing series capacitance.

shunt capacitance is varied from 0.60 pF to 1.40 pF. The simulation results are shown in Figure 6. It can be seen that the center frequency is tuned from 6.80 GHz to 5.00 GHz when the shunt capacitance varies from 0.60 pF to 1.40 pF. The center frequency shifts to 4.80 GHz when the shunt capacitance value becomes 1.80 pF. For bandwidth tuning, the shunt capacitance was fixed at 0.8 pF and the series capacitance is varied from 370 fF to 700 fF. The simulation results are shown in Figure 7. It can be seen that the bandwidth (-3 dB) is changed from 1.6 GHz to 3 GHz when the series capacitance vary from 370 fF to 700 fF.

3. FABRICATION OF THE FILTER

The prototype of the filter was fabricated using traditional parallel plate capacitors. We have used three parallel bridges for each shunt capacitance. The variation of the capacitance can be obtained by actuating individual bridge, or combination of bridges. Each shunt capacitance is a combination of two 12 μm wide (on the two sides) and one 15 μm wide (middle) shunt bridge. The width of the centre conductor for the 50 Ω transmission lines is 140 μm with a gap of 80 μm each side in CPW configuration. The thickness of the centre electrode dielectric (Si_3N_4) is 220 nm. For each series capacitance, two equal cantilevers are used in parallel. Sputtered gold was used as a suspended beam. A negative stress gradient was present in the sputtered gold. Therefore, cantilevers of different beam widths were used for the capacitance variation in the fabricated prototype. For the cantilevers the electrode length is 25 μm . Due to lack of actuation facility, we have used two sets of cantilever, each set contain two

cantilever in parallel, with width of $22\ \mu\text{m}$, $30\ \mu\text{m}$ for each prototype.

A four-mask process was used to fabricate the proposed filter. The cross-sectional view of the process flow of the capacitive bridges is shown in Figure 8. A $280\ \mu\text{m}$ thick silicon wafer with $4\text{--}8\ \text{k}\Omega\text{-cm}$ resistivity (specified by supplier) was used for the fabrication. A $500\ \text{nm}$ thick oxide was grown on the silicon wafer to reduce loss (A). Then $500\ \text{nm}$ thick aluminium layer was deposited by sputtering and patterned by wet etching (B). A $220\ \text{nm}$ thick Si_3N_4 was deposited as dielectric by plasma-enhanced chemical vapour deposition (PECVD)

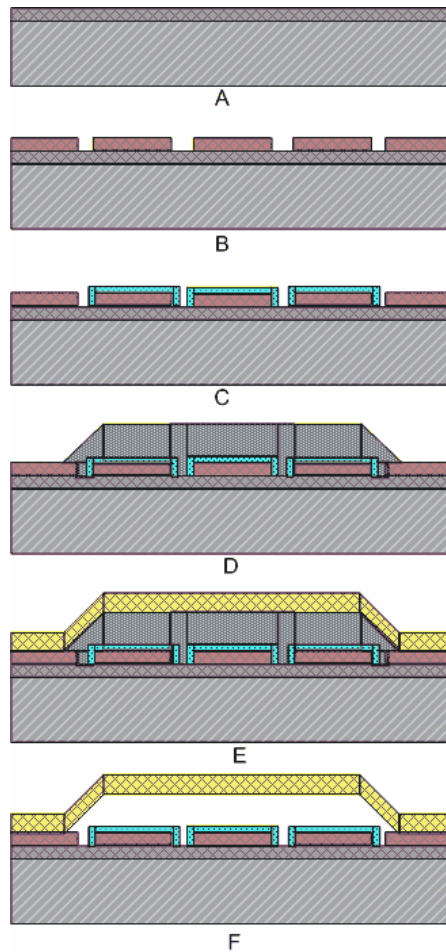


Figure 8. The 4 masks process flow for the fabrication of the band-pass filter.

and patterned by dry etch (C). HiPR 6517 photoresist was used as a sacrificial layer. The resist thickness was $2.55\ \mu\text{m}$ and patterned by standard lithography and special baking methods (D) as described in detail in [16]. Then $1.1\ \mu\text{m}$ thick gold was sputtered and patterned by wet etch (E). The gold was sputtered with very low power and a pressure of 20 m Torr to give a low tensile stress, as described in [17]. A 50 nm thick NiCr layer was used as an adhesive layer between gold and aluminium. When the gold was sputtered, the transmission line was also sputtered with $1.1\ \mu\text{m}$ additional gold on aluminum. Low tensile stress ensures a low actuation voltage and gives better reliability. Finally the switches and filters were released and dried in a critical point dryer [17].

A SEM image of the fabricated band-pass filter is shown in Figure 9. An enlarged image at the capacitance region is also shown in Figure 10. The actuation electrodes are separated from the RF signal electrode, and each bridge and cantilever have their own set of actuation electrodes. In Figure 9 the centre narrow line is the 80 Ohm transmission line, which is equivalent to a series inductor. The capacitors are at both ends of the 80 Ohm transmission line shunting a 50 Ohm transmission line. The cantilevers at the end of the bridge form the series capacitances. In the Figure 10, the three parallel bridges of shunt capacitors and the two parallel cantilevers for series capacitor can be seen. The extended 50 Ohm transmission lines are used for measurement purpose with a CPW probe.



Figure 9. A SEM image of the fabricated band-pass filter.

4. MEASURED RESULTS AND RESIMULATION CONSIDERING FABRICATION CONSTRAINTS

The fabricated filters were measured at Norwegian University of Science and Technology (NTNU), high frequency measurement lab, using a vector network analyser from Agilent. The filter characteristic

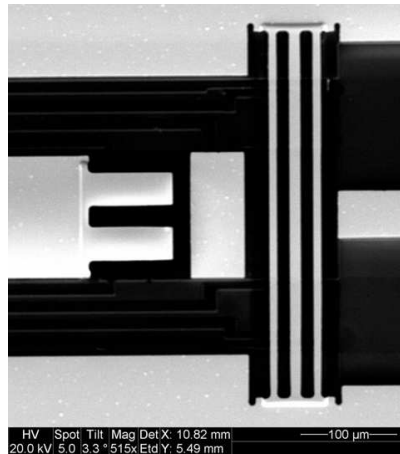


Figure 10. Enlarged SEM image of the capacitance area of the band-pass filter.

was measured up to 30 GHz. Standard Line-Reflect-Reflect-Match (LRRM) methods were used for calibration of the network analyser. The actuation voltage was around 15 volt for shunt bridge and 8 volt for cantilevers. The measured filter S parameters are shown in Figure 11. We have measured the filter characteristics with one bridge down ($15\ \mu\text{m}$ wide centre bridge) red line, and 2 bridges down ($15\ \mu\text{m}$ and $12\ \mu\text{m}$ wide bridges) blue line, both with two $22\ \mu\text{m}$ wide cantilevers down. We have also measured the band-pass filter performance with 1 bridge ($15\ \mu\text{m}$ wide) down and two $30\ \mu\text{m}$ wide cantilevers down (black line). From Figure 11, it can be seen that both center frequency and bandwidth change with shunt and series capacitance. There is an upward shift in the center frequency from the simulation results. This happened as a result of a decrease in the capacitances owing to electrode roughness, over etching, non planarity of the bridge and other non ideal effect during fabrication. These effects were considered, re-simulated the filter performance in ADS and presented below.

After fabrication the filters were inspected in an optical interferometer to measure the actual width and height of the bridge. The actual initial heights of the bridges were $2.25\ \mu\text{m}$ and the width was reduced on average $1\ \mu\text{m}$ from each side owing to over-etching. The roughness was measured in an atomic force microscopy (AFM). Gold is usually smooth and it was found that the average roughness of the gold was $7\ \text{nm}$. The Si_3N_4 average roughness was $9\ \text{nm}$ on aluminum. But the main contribution to the roughness was from aluminum. This is because of the high temp (300°C) Si_3N_4 deposition. From AFM

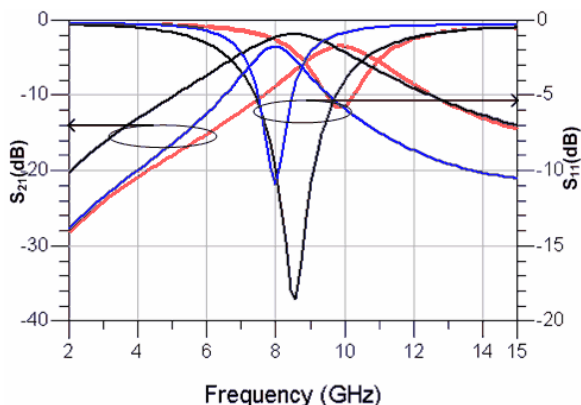


Figure 11. Measured filter responses of the fabricated band-pass filter. Red line 15 μm shunt bridge and 22 μm cantilevers down, blue line 15 and 12 μm bridge down and 22 μm cantilevers down, black line 15 μm bridge and 30 μm cantilevers down.

measurement, it was found that the height of the aluminum bumps was about 80 nm. As the nitride was deposited on aluminum, the total amplitude of roughness for the downstate capacitance was 96 nm. The dielectric constant of the Si_3N_4 is 7.5. Considering the overetch and roughness, according to Equation (4), the downstate capacitance became 0.38 pF for the 15 μm bridge (W_e , 13 μm real width) and 0.30 pF for the 12 μm bridge (W_e , 10 μm real width). In all cases, the length of the electrode, L_e was 140 μm . Using the same roughness, the downstate capacitance for a 22 μm wide cantilever beam became 0.19 pF and for 30 μm wide cantilever beam became 0.285 pF. The filter was re-simulated with the above parameters.

The tuning of center frequency and comparison between simulation and measurement results of the fabricated filter as shown in Figure 12. For one bridge down and the 22 μm wide cantilevers down, the shunt capacitance becomes 0.38 pF and total series capacitance becomes 0.38 pF (2 cantilevers in parallel). For two bridges down and the 22 μm cantilevers down, the shunt capacitance becomes 0.68 pF and the series capacitance becomes 0.38 pF. For clarity, the S_{11} is not included in the comparison and also the frequency range is reduced. It can be seen that the measured results agree well with the re-simulated results, including the effect of over-etching and roughness. There is a slightly higher center frequency in the measured filter. This can happen because of reduced capacitance owing to non-planarity of the bridge and the cantilever at downstate, which will further reduce the

downstate capacitance.

The tuning of the bandwidth and comparison between re-simulation and measurement results of the fabricated filter are shown in Figure 13. For one bridge down and the 22 μm cantilevers down, the shunt capacitance becomes 0.38 pF and the series capacitance becomes 0.38 pF (two equal cantilevers in parallel). For one bridge down and

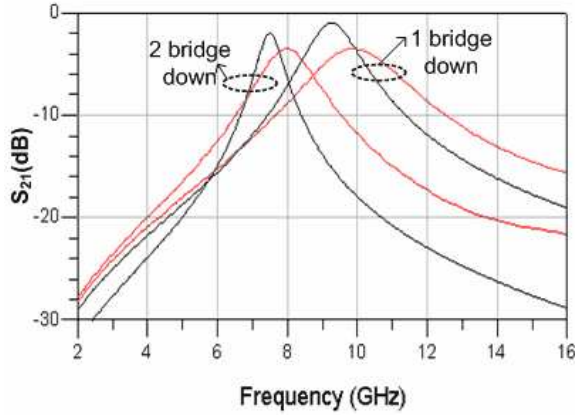


Figure 12. Comparison of filter center frequency tuning between measured response and simulation considering the effect of fabrication constraints (red line measured and black line re-simulated).

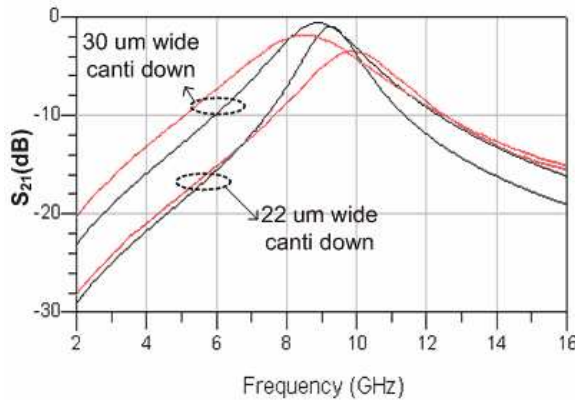


Figure 13. Comparison of filter bandwidth tuning between measured response and simulation considering the effect of fabrication constraints (red line measured and black line re-simulated).

the 30 μm cantilevers down, the shunt capacitance becomes 0.38 pF and the series capacitance becomes 0.57 pF (two equal cantilevers in parallel). From Figure 13, it can be seen that the measured results agree well with the re-simulated results, given the effect of over-etching and roughness. Again the measured filter has a slightly higher center frequency for the reason discussed above.

At high frequency an increase in insertion loss and return loss occurs in the filter performance. The smaller value of series capacitance may increase the return loss at higher center frequency. Capacitive tuning with an inductive inverter can be used to reduce the return loss for the entire tuning range [18, 19]. Simultaneous tuning of both capacitance and inductance with stub can also be used to reduce return loss and insertion loss for the entire operating range of the filter [20]. The filter roll-off is not very sharp, however can be improved by the use of a high-impedance transmission line and a higher order of the filter. As only the capacitance is used for tuning and the inductance is fixed, this will reduce the tuning range of the filter significantly.

5. CONCLUSION

We have presented a tunable band-pass filter design with transmission line and MEMS capacitances. Parallel plate capacitances were used as series and shunt capacitance and fabricated using surface micromachining technique. The tuning of the center frequency has been obtained by actuation of various parallel shunt bridges. The tuning of the band-width has been obtained by actuating different combinations of series cantilevers. The operating frequency shifted upward to some extent from the designed parameters due to reduced capacitance. The capacitance was decreased owing to roughness, over etching and non planarity of the suspended bridge. The measured results agree well with the simulated result considering the fabrication effects. The filter has the flexibility of tuning both center frequency and bandwidth simultaneously. The filter is very compact and has very good control of the tuning frequency.

ACKNOWLEDGMENT

Authors are grateful to Norwegian Research Council for sponsoring the work through SMiDA project (No. 159559/130) and IRRFT project (No. 159259/140). Authors also like to thank MiNa Lab personnel for their support in the clean room and Mr. Tjrie Martinsen from IET/NTNU for his help during S parameter measurement.

REFERENCES

1. Zou, J., C. Liu, J. Schutt-Aine, J. Chen, and S. Kang, "Development of a wide tuning range MEMS tunable capacitor for wireless communication systems," *International Electron. Devices Meet. Tech. Digest*, 403–406, 2000.
2. Afrang, S. and E. Abbaspour-Sani, "A low voltage MEMS structure for RF capacitive switches," *Progress In Electromagnetics Research*, Vol. 65, 157–167, 2006.
3. Abbaspour-Sani, E., N. Nasirzadeh, and G. R. Dadashzadeh, "Two novel structures for tunable MEMS capacitors with RF applications," *Progress In Electromagnetics Research*, Vol. 68, 169–183, 2007.
4. Topalli, K., M. Unlu, H. I. Atadoy, S. Demir, O. Aydin Civi, and T. Akin, "Empirical formulation of bridge inductance in inductively tuned RF MEMS shunt switches," *Progress In Electromagnetics Research*, Vol. 97, 343–356, 2009.
5. Liu, Y., A. Borgioli, A. S. Nagra, and R. A. York, "Distributed MEMS transmission line for tunable filter applications," *Int. J. RF and Microwave CAE*, Vol. 11, 254–260, John Wiley & Sons, Inc., 2001.
6. Tamijani, A. A., L. Dussopt, and G. M. Rebeiz, "Miniature and tunable filters using MEMS capacitors," *IEEE Transaction on Microwave Theory and Technique*, Vol. 51, No. 7, 1878–1885, Jul. 2003.
7. Peroulis, D., S. Pacheco, K. Sarabandi, and L. P. B. Katehi, "Tunable lumped components with applications to reconfigurable MEMS filters," *IEEE MTT-S Digest*, Vol. 1, 341–344, May 20–25, 2001.
8. Lee, S., J. Kim, J. Kim, Y. Kim, and Y. Kwon, "Millimeter-wave MEMS tunable low pass filter with reconfigurable series inductor and capacitive shunt switches," *IEEE Microwave and Wireless Components Letters*, Vol. 15, No. 10, 691–693, Oct. 2005.
9. Park, J., S. Lee, J. Kim, H. Kim, Y. Kim, and Y. Kwon, "Reconfigurable millimeter-wave filters using CPW-based periodic structures with novel multiple-contact MEMS switches," *IEEE Journal of Microelectromechanical Systems*, Vol. 14, No. 3, 456–463, Jun. 2005.
10. Saha, S. C. and T. Sæther, "Modeling and simulation of low pass filter using RF MEMS capacitance and transmission line," *Proceeding IMAPS Nordic*, 155–159, 2005.

11. Saha, S. C., U. Hanke, and T. Sæther, "Modeling, design and simulation of tunable band-pass filter using RF MEMS capacitance and transmission line," *SPIE International Symposium, Microelectronics, MEMS and Nanotechnology, Proc. of SPIE*, Vol. 6035, Brisbane, Australia, Dec. 2005.
12. Rebeiz, G. M., *RF MEMS Theory, Design, and Technology*, 92, John Wiley & Sons, 2003.
13. Pozar, D. M., *Microwave Engineering*, 2nd edition, Vol. 8, John Wiley & Sons, 1998.
14. Chiou, Y.-C. and J.-T. Kuo, "Planar multiband bandpass filter with multimode stepped-impedance resonators," *Progress In Electromagnetics Research*, Vol. 114, 129–144, 2011.
15. Advance Design Systems (ADS) from Agilent.
16. Saha, S. C., H. Sagberg, E. Poppe, G. U. Jensen, T. A. Fjeldly, and T. Sæther, "Tuning of resist slope with hardbaking parameters and release methods of extra hard photoresist for RF MEMS switches," *Journal of Sensor and Actuators A: Phys.*, Vol. 142, 452–461, 2008.
17. Saha, S. C., H. Sagberg, E. Poppe, G. U. Jensen, and T. Sæther, "Metallization scheme and release methods for fabrication of RF MEMS switches," *Proceedings of 33rd Micro- and Nano-Engineering Conference (MNE 2007)*, Copenhagen, Denmark, Sep. 2007.
18. Entesari, K. and G. M. Rebeiz, "A differential 4-bit 6.5–10 GHz RF MEMS tunable filter," *IEEE Transaction of Microwave Theory and Techniques*, Vol. 53, No. 3, Part 2, 1103–1110, 2005.
19. Matthaei, G. L., E. Young, and E. M. T. Jones, *Microwave Filters, Impedance-Matching Networks, and Coupling Structures*, Artech House, Norwood, MA, 1980.
20. Pillans, B., A. Malczewski, R. Allison, and J. Brank, "6–15 GHz RF MEMS tunable filters," *IEEE MTT-S*, 919–922, 2005.